Çukurova Üniversitesi Mühendislik Mimarlık Fakültesi Dergisi, 26(2), ss. 105-117, Aralık 2011
Çukurova University Journal of the Faculty of Engineering and Architecture, 26(2), pp.105-117, December2011

Effects of the Boundary Conditions on the Numerical Solution of the Orifice Flow**

Tural TUNAY*[1], Beşir ŞAHİN[1] ve Ali KAHRAMAN[2]
[1] Çukurova Üniversitesi, Müh. Mim. Fak., Makine Mühendisliği Bölümü, Adana
[2] Selçuk Üniversitesi, Teknik Eğitim Fakültesi, Makina Eğitimi Bölümü, Selçuklu, Konya

Abstract

The present study is primarily aimed at the effects of boundary conditions on the numerical solutions of the laminar flow characteristics through an orifice plate inserted in a pipe with the aid of vorticity-transport equations. For this purpose, orifice discharge coefficient was used as a main flow parameter. Discretization of vorticity-transport equations was made by using alternating direction implicit method. Two different boundary conditions were used to calculate vorticity values at the pipe walls and also three different boundary conditions were used to find vorticity values at the orifice corner points. The ratio of orifice diameter to the pipe diameter, β=0.6, was kept constant and dimensionless orifice plate thickness L^* was selected as 1/12. The fluid flow was assumed to be two dimensional, axisymmetric, viscous, incompressible, steady, fully developed and laminar.

Key words: Boundary conditions, discharge coefficient, laminar flow, orifice meter, vorticity transport equations.

Orifis Etrafındaki Akışın Sayısal Yöntemlerle Çözümüne Sınır Şartlarının Etkisi

Özet

Bu çalışmada sınır şartlarının boru içerisine yerleştirilmiş orifis metre etrafındaki laminar akış yapısının, girdap-transport denklemleri yardımıyla, sayısal yöntem kullanılarak çözümüne etkisinin incelenmesi amaçlanmıştır. Bu amaç doğrultusunda orifis debi çıkış katsayısı ana parametre olarak kullanılmıştır. Girdap transport denklemlerinin ayrıklaştırılması implisit değişen yönler yöntemi kullanılarak yapılmıştır. Boru cidarında girdap değerlerini hesaplamak için iki farklı sınır şartı ve orifis metre köşe noktalarında girdap değerlerini hesaplamak için ise üç farklı sınır şartı kullanılmıştır. Orifis çapının boru çapına oranı sabit olup, β=0.6 'dır ve boyutsuz orifis kalınlığının değeri, L^*, ise 1/12'dir. Akış iki boyutlu, eksenel simetrik, viskoz, sıkıştırılamaz, daimi, tam gelişmiş ve laminar kabul edilmiştir

Anahtar Kelimeler: Sınır şartları, debi çıkış katsayısı, laminar akış, orifis metre, girdap transport denklemleri.

* Yazışmaların yapılacağı yazar: Tural Tunay, *Çukurova Üniversitesi, Müh. Mim. Fak., Makine Mühendisliği Bölümü, Adana*. ttunay@cu.edu.tr

** This paper is revised and updated form of the paper presented in "Proceeding of the Fourth GAP Engineering Congress" which is organised through 6-8 June 2002

1. INTRODUCTION

Flow rate measurement of fluid flow is of great importance everywhere in industry. Because the quantity of fluid flowing through pipes must be known precisely in order to have economically optimum operations. As it is known that the orifice meter is one of the most frequently used flow measurement devices in industry. For this reason, measurement of flow rate obtained by using this device should be accurate. An error in metering the flow rate may cause substantial economic losses. For example, according to the statement of Morrison et al. [1], in USA one million orifices are used and because of the wrong measurements, large amount of economical losses occur per year. Considerable research efforts in the study of orifice flow have been devoted to applications involving flow meters. These orifices typically have diameter ratios (β) in the range of 0.2 to 0.75 and orifice thickness/diameter ratios (L^*) less than 1 [2,3,19,22,23].

In laminar flow, the variation of discharge coefficient (C_d) is substantially rapid with the orifice thickness/diameter ratio (L^*), orifice/pipe diameter ratio (β) and Reynolds number (Re). It is known from the previous studies conducted on the orifice flow [3,13,14], the values of discharge coefficients change rapidly until $Re_d \leq 150$. After this level of Reynolds number, the value of discharge coefficient varies approximately in between C_d= 0.72~0.77 for β=0.6 [3].

Johansen [4] examined the characteristics of flow through orifice plate in two series of experiments. In the first group, he made visual observations of the flow of water through orifices in a glass pipe by means of colouring matter injected into the stream. Photographs were also taken illustrating a number of typical conditions of flow sufficient to define the transitions leading to the establishment of complete turbulence. In this part of experiments, four sizes of orifice (d_o/D = 0.1, 0.25, 0.5, 0.75) were used and he observed similar flow characteristics in each case. In the second series of Johansen's experiments, orifices were mounted in a length of smooth brass pipe and the discharge coefficients determined down to values of Reynolds number. In his pressure experiments, he determined the relation between the discharge through a pipe orifice and the differential head across the diaphragm for a series of sharp-edged orifices (d_o/D = 0.209, 0.400, 0.595, 0.794) over a range of Reynolds numbers extending from over 25000 down to less than unity. He used orifices of similar shape in both series of experiments. They were sharp edged, and bevelled at 45^o on the downstream side.

An extensive experimental work has been carried out by Alvi et al. [5] on the loss characteristics and discharge coefficient of the sharp-edged orifices, quadrant-edged orifices and nozzles for Reynolds numbers in the range of $20 \leq Re_d \leq 10^4$ with varying β, keeping the orifice thickness/diameter ratio (L^*) constant. A numerical algorithm for the solution of steady, viscous flow through a pipe orifice that allows a considerable flexibility in the choice of orifice plate geometry with a constant thickness has been discussed by Nigro et al. [6].

The description of the steady flow of an incompressible fluid through the orifice has been semi-empirically established for only certain flow conditions by Grose [7]. He has shown that the discharge coefficient was solely dependent upon the viscosity coefficient for Re_0 less than 16. Nallasamy [8] has studied the characteristics of the separated flow behind the obstacle for Re_0 values in the range of $0 < Re_0 \leq 1500$. He has examined the effects of thickness and height of the obstacle and the inlet velocity profile on the separated flow region.

Numerical solution of Navier-Stokes equations has been obtained by Mills [9] for Re_o values in the range of $0<Re_o \leq 50$ having steady, axisymmetric, viscous, incompressible fluid flow with a fixed orifice/pipe diameter ratio of β=0.5 and a fixed orifice thickness/diameter ratio L^*. Mills [9] has stated that in view of the axisymmetric nature of the flow, it was no longer possible to use the same boundary conditions for both vertical and horizontal walls as can be assumed for two-dimensional flow referred to a rectangular coordinate system.

Coder and Buckley [10] have presented a

technique for the numerical solution of the unsteady Navier-Stokes equations for laminar flow through the orifice plate within a pipe. They accomplished the solution through the rearrangement of the equations of motion into a vorticity transport equation and a definition-of-vorticity equation, which are solved by an implicit numerical method. They used an equation, which is proposed by Lester [11] to find vorticity on the pipe wall and orifice surface. In the present work, this equation was also used as a first boundary condition to obtain vorticity values on the pipe wall.

Ma and Ruth [12] have presented a new numerical technique for treating the vorticity singularity of incompressible viscous flow around a re-entrant sharp corner. They have developed vorticity circulation method for contracting flow, which is characterized by the local flow acceleration and separation. They used boundary condition for vorticity, which was found by considering the continuity and no-slip constraints at the fluid/solid interface. In the present work, this boundary condition was also used as a second boundary condition to find vorticity values at the pipe wall.

Şahin and Ceyhan [13] have investigated the flow characteristics through the square-edged orifice inserted in the pipe both numerically and experimentally. In their study, they have solved the governing equations by assuming the flow is steady, fully developed, laminar, incompressible, two-dimensional and axisymmetric with Reynolds numbers in the range of $0<Re_o\leq 144$ and orifice thickness/diameter ratio in the range of $1/16\leq L^*\leq 1$. They have observed that the length of the separated flow region changes rapidly especially at low Reynolds numbers.

By considering the same flow geometry and assumptions, Şahin and Akıllı [14] have investigated the flow characteristics such as the length of separated flow region, velocity vectors, contours of stream function. They used finite element method having the Reynolds numbers in the range of $0<Re_o\leq 2000$, orifice thickness/diameter ratio in the range of $1/16\leq L^*\leq 1$ and orifice/pipe diameter ratio in the range of $0.2 \leq \beta \leq 0.9$ in their study.

A study of laminar pulsating flow through a 45-degree beveled pipe orifice has been performed using finite difference approximations to the governing stream function and vorticity transport equations by Jones and Bajura [15]. They have obtained the solution for β values varying from 0.2 to 0.5 with Re_0 values in the range $0 < Re_0 \leq 64$.

Gan and Riffat [16] have conducted a study on the pressure loss characteristics of square edged orifice and perforated plates. They have carried out tests to determine the pressure loss coefficient for thin plates in a square duct for a range of Reynolds numbers. They have used computational fluid dynamics (CFD) to predict the loss coefficient, and their results were compared with experimental results. They have conducted studies to understand the effect of plate thickness on the loss coefficient for the orifice plate using CFD.

Ramamurthi and Nandakumar [17] conducted studies on the discharge coefficients for flow through small sharp-edged cylindrical orifices of diameters between 0.3 mm and 2 mm and aspect ratios between 1 and 50. They determined the characteristics of flow in the separated, attached and cavitated flow regions. They have shown that while the discharge coefficient scales with the Reynolds number and aspect ratio in the attached flow regions, the diameter influences the discharge coefficient in the separated flow region. They have indicated that the onset of cavitation in the orifice is dependent on the diameter and aspect ratio. They have also stated that the values of discharge coefficients for separated and cavitated flows do not depend on Reynolds number. The critical cavitation number is also dependent on the diameter and the aspect ratio of the orifice.

Huang and Seymour [18] have investigated the effect of a corner singularity on the accuracy of the finite difference solution to the incompressible viscous flow equations. They have considered two problems that include corner singularities. The first concerned the flow of a viscous fluid in a channel driven by a constant pressure gradient, when the velocity satisfies a two-dimensional Poisson equation. The second was Stokes flow in a two-dimensional region when the stream-function satisfies the biharmonic equation. For both

problems the boundaries of the domains contain corners. They stated that the stress or the vorticity is singular for corner angles greater than some critical value. They have shown that numerical approximations for the stream-function and velocity converge to the exact solutions despite the corner singularities using both a formal analysis and numerical results.

Mishra et al. [19] have experimentally investigated various characteristics of the incompressible and compressible flows through rectangular microorifices entrenched in microchannels. Their discharge coefficient results in incompressible flow matches the results obtained at the macroscale. For the incompressible flows through microdevices a correlation estimating the discharge coefficient was provided. They have observed that the flow rate is controlled by the constriction element area rather than the microchannel area for the compressible flows through microdevices.

Zimmermann [20] has conducted experiments to examine the influence of a disturbed pipe flow on the flow coefficient of a standard orifice plate. He presented that the existing standard should be revised as regards the definition of the fully developed turbulent flow profile and the selection of the required upstream lengths.

The present study is primarily aimed at the effects of boundary conditions on the numerical solutions of the laminar flow characteristics through the orifice plate inserted in a pipe with the aid of vorticity-transport equation. By using vorticity-transport equation, the mixed elliptic-parabolic Navier Stokes equations have been separated into one parabolic and one elliptic equation. This procedure requires that appropriate expressions for vorticity (ω) and stream function (ψ) be specified at the boundaries. The stability and accuracy of the solution depends on these boundary conditions. Although the governing equations are the same for all type of fluid flow geometries, the differences appearing in the numerical solution of governing equations of fluid flow come through the initial and boundary conditions [21]. Because of this reason, it is substantially important to use consistent boundary conditions in order to have accurate numerical solutions. The orifice flow, which has mathematically singular points and no-slip boundary condition for the vorticity, is the special case for the present numerical studies with the aid of vorticity-transport equations.

Governing equations was solved by means of a marching technique called alternating direction implicit method. A computer code in FORTRAN language was developed for that purpose. Flow was assumed to be fully-developed, incompressible, viscous, axisymetric, steady and laminar. Orifice/pipe diameter ratio β, which is 0.6 and orifice thickness/diameter ratio L^*, which is 1/12, were kept constant throughout the calculations.

2. GEOMETRY OF FLOW WITH OBSTACLE

The square-edged orifice plate inserted in a circular pipe is shown in Figure 1. In this figure, cross sections 1 and 2 represent the locations of pressure taps used for the numerical calculation of the orifice discharge coefficient. The length between the location of the upstream tapping point and the inlet surface of the orifice was one diameter of the pipe, D. The length between the downstream pressure tapping and the inlet surface of the orifice was one half of the pipe diameter, D/2. Because fully developed flow condition was assumed at the inlet of the pipe, an orifice plate which is placed 4D from the inlet and 23D from the exit of the pipe was used as shown in Figure 3. The orifice plate used has a concentric hole.

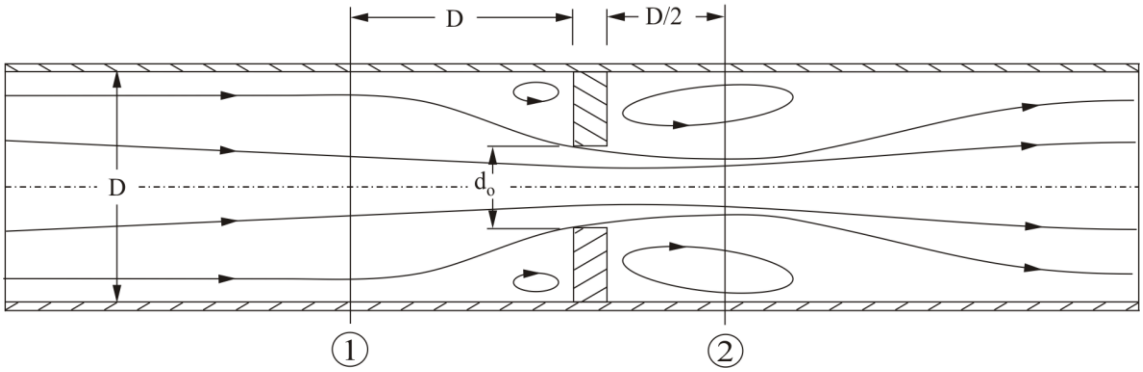

Figure 1. Square-edged orifice meter inserted in a circular pipe

A grid independency study was performed to find a grid that was sufficiently fine to provide accurate solutions. In order to check the grid independency of the computation, predictions of the discharge coefficient with various size of the mesh inserted in the flow field at a Reynolds number of 400 was carried out. Comparison of the discharge coefficient for different grid sizes is given in Figure 2. As seen from Figure 2, the value of orifice discharge coefficient does not change considerably by increasing number of nodes from 56x3024 to higher values. So that, for the investigation of flow characteristics, the flow field was divided into 56 intervals in the vertical direction and 3024 intervals in the horizontal direction.

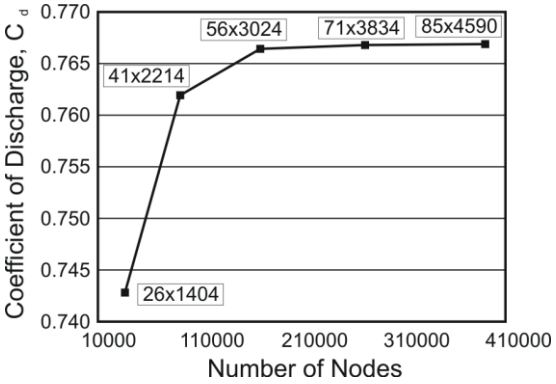

Figure 2. Variation of the orifice discharge coefficient with various mesh sizes at the Reynolds Number of 400

As it is well known that the orifice discharge coefficient is a function of the orifice thickness/diameter ratio (L^*), orifice/pipe diameter ratio (β) and Reynolds number (Re). In practice, the accuracy of the measurement of the volume flow rate strongly depends on the accurate measurement of the pressure differential, which is caused by the orifice plate. The relationship between the pressure differential and the volume flow rate can be characterized by the discharge coefficient (C_d). The orifice discharge coefficient for steady flow has been defined by applying the continuity and Bernoulli equations to flow geometry shown in Figure 1.

$$C_d = \frac{1}{2\sqrt{2}}\left(\frac{1}{\beta}\right)^2\left(1-\beta^4\right)^{1/2}\frac{1}{\sqrt{\Delta P^*}} \qquad (1)$$

Here ΔP^* is the dimensionless pressure difference between cross sections 1 and 2 shown in Figure 1.

3. MATERIAL AND METHODS

In this study, flow was assumed to be steady, viscous, fully developed, incompressible, laminar and axisymmetric. Equations governing this type of flow are expressed as follows;

Navier-Stokes equations;

$$\frac{\partial V_r}{\partial t}+V_r\frac{\partial V_r}{\partial r}+V_z\frac{\partial V_r}{\partial z}=-\frac{1}{\rho}\frac{\partial P}{\partial r}+\nu\left(\frac{\partial^2 V_r}{\partial r^2}+\frac{1}{r}\frac{\partial V_r}{\partial r}-\frac{V_r}{r^2}+\frac{\partial^2 V_r}{\partial z^2}\right) \qquad (2.a)$$

$$\frac{\partial V_z}{\partial t}+V_r\frac{\partial V_z}{\partial r}+V_z\frac{\partial V_z}{\partial z}=-\frac{1}{\rho}\frac{\partial P}{\partial z}+\nu\left(\frac{\partial^2 V_z}{\partial r^2}+\frac{1}{r}\frac{\partial V_z}{\partial r}+\frac{\partial^2 V_z}{\partial z^2}\right) \qquad (2.b)$$

Continuity equation;

$$\frac{\partial V_r}{\partial r}+\frac{V_r}{r}+\frac{\partial V_z}{\partial z}=0 \tag{3}$$

On the other hand, since we investigate steady flow, time derivative in equations (2) should be taken as zero. But, in this case, vorticity transport equation obtained becomes nonlinear and elliptic partial differential equation. Because of the fact that stability can be obtained more quickly with parabolic equations, the time derivative of velocity components was left in equations (2) consciously. In this way, an elliptic type equation was converted into parabolic type equation. This addition of term has no physical meaning. Velocity components of the flow are expressed in terms of stream function as follows,

$$V_r=\frac{1}{r}\frac{\partial \psi}{\partial z} \tag{4}$$

$$V_z=-\frac{1}{r}\frac{\partial \psi}{\partial r} \tag{5}$$

Following group of dimensionless parameters was used to obtain dimensionless form of the governing equations.

$$V_r^*=\frac{V_r}{\overline{V}},\ V_z^*=\frac{V_z}{\overline{V}},\ z^*=\frac{z}{R},$$
$$r^*=\frac{r}{R},\ Re_d=\frac{\rho\overline{V}(2R)}{\mu},$$
$$P^*=\frac{P}{\frac{1}{2}\rho(2\overline{V})^2},\ \psi^*=\frac{\psi}{\overline{V}R^2},\ \omega^*=\frac{\omega R}{\overline{V}},\ \tag{6}$$
$$t^*=\frac{t\overline{V}}{R}$$

Vorticity transport equation (7) and stream function equation (8) can be written as follow by using governing equations (2.a, 2.b, 4 and 5) and the group of dimensionless parameters (6) shown above.

$$\frac{\partial^2\omega^*}{\partial r^{*2}}+\frac{\partial^2\omega^*}{\partial z^{*2}}=\frac{1}{r^*}\left(\frac{\omega^*}{r^*}-\frac{\partial\omega^*}{\partial r^*}\right)+\frac{Re_d}{2}\left(\frac{\partial\omega^*}{\partial t^*}+\frac{1}{r^*}\frac{\partial\psi^*}{\partial z^*}\frac{\partial\omega^*}{\partial r^*}-\frac{1}{r^*}\frac{\partial\psi^*}{\partial r^*}\frac{\partial\omega^*}{\partial z^*}-\frac{\omega^*}{r^{*2}}\frac{\partial\psi^*}{\partial z^*}\right) \tag{7}$$

$$\frac{\partial^2\psi^*}{\partial r^{*2}}+\frac{\partial^2\psi^*}{\partial z^{*2}}=r^*\omega^*+\frac{1}{r^*}\frac{\partial\psi^*}{\partial r^*} \tag{8}$$

For the calculation of discharge coefficient, the static pressure distribution along the pipe should be calculated. Pressure distributions can be determined by integrating the dimensionless form of Navier-Stokes equations shown below with the aid of Simpson's 1/3 integration rule.

$$2\frac{\partial P^*}{\partial r^*}=\frac{2}{Re_d}\left(\frac{\partial^2V_r^*}{\partial r^{*2}}+\frac{1}{r^*}\frac{\partial V_r^*}{\partial r^*}-\frac{V_r^*}{r^{*2}}+\frac{\partial^2V_r^*}{\partial z^{*2}}\right)-\left(V_r^*\frac{\partial V_r^*}{\partial r^*}+V_z^*\frac{\partial V_r^*}{\partial z^*}\right) \tag{9}$$

$$2\frac{\partial P^*}{\partial z^*}=\frac{2}{Re_d}\left(\frac{\partial^2V_z^*}{\partial r^{*2}}+\frac{1}{r^*}\frac{\partial V_z^*}{\partial r^*}+\frac{\partial^2V_z^*}{\partial z^{*2}}\right)-\left(V_r^*\frac{\partial V_z^*}{\partial r^*}+V_z^*\frac{\partial V_z^*}{\partial z^*}\right) \tag{10}$$

4. DISCRETIZATION OF VORTICITY TRANSPORT EQUATIONS

Notations for the determination of the flow geometry and boundary conditions were given in Figures 3 and 4. Here, (i) and (j) notations were used for terms in axial and radial directions, respectively. Pressure values, which were necessary for the calculation of discharge coefficient, were taken from the cross sections D-D/2 as shown in Figure 1.

Equation (7) was solved by means of a marching technique called alternating direction implicit method (ADI). In this method, values of $\omega^*(t+\Delta t)$ were obtained in some fashion from the known values of $\omega^*(t)$. The solution of $\omega^*(t+\Delta t)$ was achieved in a two step process, where intermediate values of ω^* were found at an intermediate time,

(t+ Δ t/2). In the first step, over a time interval Δt/2, the spatial derivatives in equation (7) were replaced with central differences, where only the z derivative was treated implicitly and the following equation was yielded;

$$\frac{Re_d}{2}\frac{\omega^{*n+1/2}_{i,j}-\omega^{*n}_{i,j}}{\Delta t^*/2}+\frac{Re_d}{2}V^{*n}_r\frac{\omega^{*n}_{i,j+1}-\omega^{*n}_{i,j-1}}{2H}+\frac{Re_d}{2}V^{*n}_z\frac{\omega^{*n+1/2}_{i+1,j}-\omega^{*n+1/2}_{i-1,j}}{2H}-\frac{Re_d}{2}\frac{V^*_r}{r^*}\omega^{*n+1/2}_{i,j}$$
$$=\frac{\omega^{*n}_{i,j-1}-2\omega^{*n}_{i,j}+\omega^{*n}_{i,j+1}}{H^2}+\frac{\omega^{*n+1/2}_{i-1,j}-2\omega^{*n+1/2}_{i,j}+\omega^{*n+1/2}_{i+1,j}}{H^2}-\frac{\omega^{*n+1/2}_{i,j}}{r^{*2}}+\frac{1}{r^*}\frac{\omega^{*n}_{i,j+1}-\omega^{*n}_{i,j-1}}{2H} \quad (11)$$

The second step of the alternating direction implicit method scheme took the solutions of ω^* for time t+Δt, using the known values at time t+Δt/2. For this second step, the spatial derivatives in equation (7) were replaced with central differences, where the r derivative was treated implicitly. Hence, equation (7) can be presented as;

$$\frac{Re_d}{2}\frac{\omega^{*n+1}_{i,j}-\omega^{*n+1/2}_{i,j}}{\Delta t^*/2}+\frac{Re_d}{2}V^{*n}_r\frac{\omega^{*n+1}_{i,j+1}-\omega^{*n+1}_{i,j-1}}{2H}+\frac{Re_d}{2}V^{*n}_z\frac{\omega^{*n+1/2}_{i+1,j}-\omega^{*n+1/2}_{i-1,j}}{2H}-\frac{Re_d}{2}\frac{V^*_r}{r^*}\omega^{*n+1}_{i,j}$$
$$=\frac{\omega^{*n+1}_{i,j-1}-2\omega^{*n+1}_{i,j}+\omega^{*n+1}_{i,j+1}}{H^2}+\frac{\omega^{*n+1/2}_{i-1,j}-2\omega^{*n+1/2}_{i,j}+\omega^{*n+1/2}_{i+1,j}}{H^2}-\frac{\omega^{*n+1}_{i,j}}{r^{*2}}+\frac{1}{r^*}\frac{\omega^{*n+1}_{i,j+1}-\omega^{*n+1}_{i,j-1}}{2H} \quad (12)$$

Equation (11) and (12) can be reduced to three diagonal matrix forms. Stream function equation was solved with the aid of successive relaxation method as follow;

$$\psi^{*n+1}_{i,j}=0.25\left(\psi^*_{i+1,j}+\psi^*_{i-1,j}+\psi^*_{i,j-1}+\psi_{i,j+1}\right)-\frac{H}{8r^*_j}\left(\psi^*_{i,j+1}-\psi^*_{i,j-1}\right)+\frac{H^2r^*_j}{4}\omega^*_{i,j} \quad (13)$$

5. INITIAL AND BOUNDARY CONDITIONS

For the velocity values at the pipe walls, no slip boundary condition is applied. At the inlet of the pipe (AB), flow is assumed to be fully developed. Since the flow is axisymmetric, radial velocity component should be zero along the centreline of the pipe (AH). Therefore, the value of stream function through the centreline becomes constant. If above conditions are satisfied, the value of stream function on the pipe wall (through BC, CI, IE, EF and FG) should also be constant. The following equation for the stream function can be written as the inlet boundary condition for laminar fully developed flow.

$$\psi^* = r^{*2}\left(1-\frac{r^{*2}}{2}\right) \quad (14)$$

Here, equation (14) can be used for the calculation of stream function at the cross section AB. On the boundaries BC, CI, IE, EF and FG, the value of stream function becomes $\psi^* = 0.5$. On the central axis, the value of stream function is equal to zero. The resulting equation for the vorticity at the inlet becomes;

$$\omega^* = 4r^* \quad (15)$$

According to this equation, vorticitiy value at the centreline (AH) is zero. At outlet (GH) derivatives of all flow variables are taken to be equal to zero.

5.1. Vorticity Values at the Pipe Walls

The flow of an incompressible fluid around a re-entrant sharp corner is encountered in many engineering problems. A typical example is the orifice inserted pipe flow. It is well known that corner points are mathematically singular points for the vorticity and pressure fields because of the no-slip boundary condition on the fluid/solid interface [12].

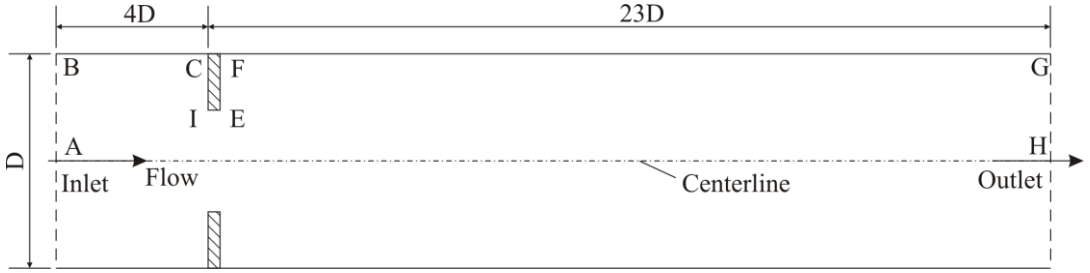

Figure 3. The simulated pipe geometry and notation for the boundary conditions

Mills [9] has commented that the same boundary condition cannot be used to calculate vorticity values for both vertical and horizontal walls for axisymmetric flow conditions. Lester [11] has considered vertical and horizontal walls separately for his calculations of the flow characteristics around orifice.

Two different boundary conditions are used to calculate vorticity values at the pipe walls in this study. The first one (BCW_1), which is derived by Lester [11], can be given as follows;

For horizontal wall;

$$\omega^*_{i,j} = \frac{\dfrac{6}{H^2 r_i^*}\left(\psi^*_{i\pm1,j} - \psi^*_{i,j}\right) - \dfrac{r^*_{i\pm1}}{r^*_i}\omega^*_{i\pm1,j}}{2 \mp \dfrac{H}{r^*_i} - \dfrac{H^2}{4 r^{*2}_i}} \qquad (16)$$

For vertical wall;

$$\omega^*_{i,j} = \frac{3}{H^2 r_i^*}\left(\psi^*_{i,j\pm1} - \psi^*_{i,j}\right) - \frac{1}{2}\omega^*_{i,j\pm1} \qquad (17)$$

Second boundary condition (BCW_2) can be obtained by considering the no-slip boundary condition at walls. Using the boundary BC as an example shown in Figure 3, we can expand $\psi^*_{i,j-1}$ by applying Taylor series using the wall values of stream function, $\psi^*_{i,j}$. Regardless of the wall orientation or boundary value of ψ^*, vorticity value at the pipe wall can be written as follow;

$$\omega^*_{i,j} = \frac{2}{r_i^*}\frac{\left(\psi^*_w - \psi^*_{w-1}\right)}{H^2} + 0(\Delta H) \qquad (18)$$

where H is the distance from (w) to (w-1), normal to the wall.

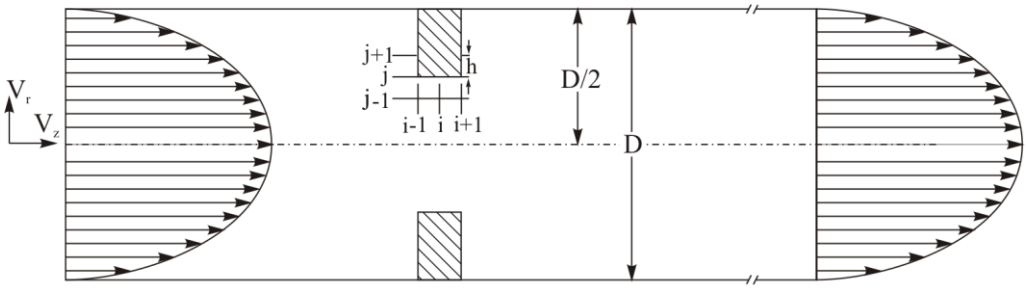

Figure 4. Flow geometry

5.2. Corner Treatments of Vorticity

The need for the corner vorticity (ω^*_c) arises from the use of finite difference approximation for vorticity values at the neighbouring points. However, there are several alternatives for the evaluation of ω_c. The no-slip wall condition for vorticity (ω^*_w) can be applied in a number of ways to calculate the value of ω^*_c. In this study, only the first order formulations for ω_c were considered, consistent with the wall equation (18). Three different methods were used for handling the value of orifice corner vorticity. These are:

1 - Discontinuous Values of Vorticity (DVV): Referring to Figure 5, two different vorticity values ω_a and ω_b are calculated by

$$\omega_a^* = \frac{2}{r_{jc}^*}\frac{\psi_{ic,jc}^* - \psi_{ic-1,jc}^*}{H^2} \quad (19)$$

and

$$\omega_b^* = \frac{2}{r_{jc}^*}\frac{\psi_{ic,jc}^* - \psi_{ic,jc-1}^*}{H^2} \quad (20)$$

respectively.

When the corner vorticity ω_c^* is applied in a difference equation about node C just upstream of the contraction, $\omega_c^* = \omega_a^*$ is used, however, $\omega_c^* = \omega_b^*$ is employed for the case of downstream calculations of node (ic,jc).

2 - Average of the Wall Vorticity Values (AWV): A single corner vorticity equal to the average of two wall values is used in this method which is presented as;

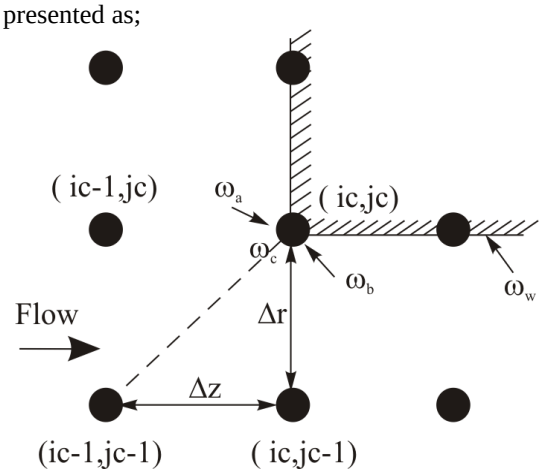

Figure 5. Notations used for the calculation of the vorticity values at the corner points of the orifice plate

$$\omega_c^* = \frac{\omega_a^* + \omega_b^*}{2} = \frac{\psi_{ic,jc}^* - \psi_{ic-1,jc}^*}{r_{jc}^* H^2} + \frac{\psi_{ic,jc}^* - \psi_{ic,jc-1}^*}{r_{jc}^* H^2} \quad (21)$$

3 - ψ - Symmetry About the Corner Point (SCP): Assuming the stream function is symmetric about the corner point, i.e. $\psi_{ic-1,jc}^* = \psi_{ic+1,jc}^*$ and $\psi_{ic,jc-1}^* = \psi_{ic,jc+1}^*$, the corner vorticity is then evaluated from;

$$\omega_c^* = \frac{2}{r_{jc}^*}\left(\frac{\psi_{ic,jc}^* - \psi_{ic-1,jc}^*}{H^2} + \frac{\psi_{ic,jc}^* - \psi_{ic,jc-1}^*}{H^2}\right) \quad (22)$$

6. RESULTS AND DISCUSSIONS

In this work, the effects of the various types of boundary conditions, which were used to calculate vorticity values at the solid boundaries and orifice corner points, on the numerical solution of the orifice flow were investigated. For this purpose, five different boundary conditions were used. Two of them were used in order to calculate the vorticity values at the pipe walls and the last three boundary conditions were used for the calculation of vorticity values at the orifice corner points.

Vorticity transport equation has been solved by using alternating direction implicit method. Numerical results obtained in the present work were compared with the mean values of experimental results taken from the open literature.

The need for the calculation of vorticity values at no-slip boundaries arises from the use of vorticity transport equation method for the solution of governing equations. Because, vorticity transport equation is solved directly in terms of two variables, which are vorticity and stream function. The corner points of the orifice plate are mathematically singular points for the vorticity and pressure fields. Because of this reason, various types of boundary conditions derived in different ways are suggested to calculate vorticity values at the solid boundaries and mathematically singular points.

Notations used for the boundary conditions in this study are as follows: i) BCW_1: The first boundary condition used to find vorticity values at the pipe wall which is given by equation (16) and (17), ii) BCW_2: The second boundary condition used to find vorticity values at the pipe wall which is given by equation (18), iii) DVV: "Discontinuous value of vorticity" method used for calculation of the vorticity values at the orifice corner points and

given by equation (19) and (20), iv) AWV: "Average value of vorticity" method used for calculation of the vorticity values at the orifice corner points and given by equation (21), v) SCP: "ψ-symmetry condition about the corner points" method used for the calculation of the vorticity values at the orifice corner points and given by equation (22).

Due to the rapid change of flow characteristics, the flow through the orifice plate were investigated for Reynolds numbers in the range of $0<Re_d \leq 1000$. It was seen that the boundary conditions are important parameters to which attention should be given. Therefore, the variations of discharge coefficient as a function of Reynolds number are calculated by using five different boundary conditions. These results are presented in Figures 6a and 6b. In these figures, while the boundary condition used for the calculation of vorticity values at the pipe wall is kept constant, the boundary condition used for the calculation of vorticity values at the orifice corner points is changed. Comparison of the results obtained by using combination of boundary conditions (AWV, SCP, DVV) used for the orifice corner points and boundary condition (BCW_1) given in equations (16) and (17), with the experimental results of Johansen [4] is shown in Figure 6a. As seen in this figure, the boundary condition that shows the best conformity with the experimental results is the combination of BCW_1 and AWV.

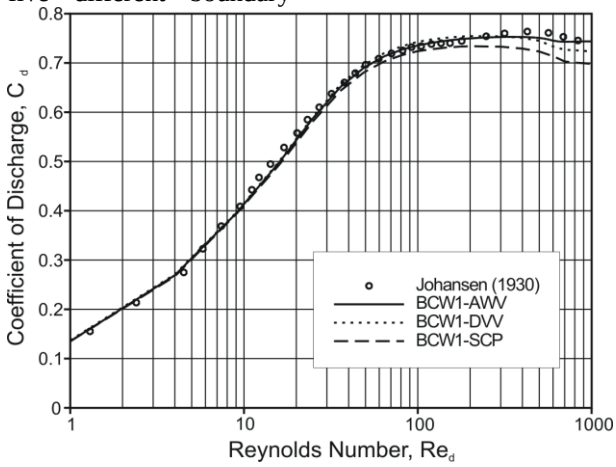

(a)

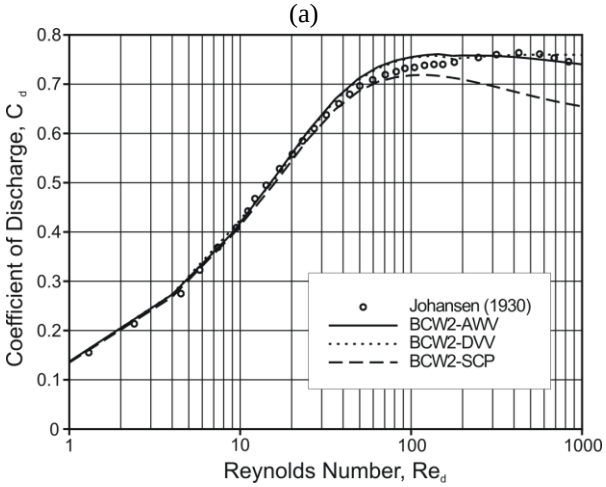

(b)

Figure 6. Variation of orifice discharge coefficient with Reynolds number for various boundary condition combinations

In addition to that, the results of other combined boundary conditions have a good agreement with the previous experimental results of Johansen [4] for Reynolds numbers $Re_d \leq 200$. At higher values of Reynolds numbers such as $Re_d>200$, the largest difference between numerically obtained results and experimental results is approximately 6%. Numerical results obtained by using BCW_2, AWV, SCP and DVV were compared with experimental results as shown in Figure 6b. Here, it is seen that the best conformity is given by the combination of boundary conditions BCW_2 and AWV. However, the maximum difference between the results of these combination of boundary conditions and experimental results of Johansen [4] is nearly 3% for the range of Reynolds numbers $30 \leq Re_d \leq 110$. In addition, the combination of SCP boundary condition with BCW_2 gives the most lack of conformity by the rate of 9% difference with the previous experimental results for the range of $200 \leq Re_d \leq 1000$. If Figures 6a and 6b are considered together, it is observed that the most suitable method for the calculation of vorticity values at the corner points of orifice is the average value of vorticity method (AWV).

By considering Figures 6a and 6b together, the best method for the calculation of vorticity values at the pipe wall can be evaluated. Results obtained by using combinations of AWV with BCW_1 and BCW_2 boundary conditions presents good agreement with the experimental results in all ranges of Reynolds numbers considered. In addition, the present numerical results obtained with the combination of SCP with BCW_1 and BCW_2 boundary conditions are also in a good agreement with previous experimental results at low Reynolds numbers in the range $0 < Re_d < 100$. But, as the Reynolds number increases this agreement becomes deteriorated. Additionally, combination of BCW_1-SCP boundary conditions gives better results than the combination of BCW_2-SCP boundary conditions. Finally, combinations of boundary conditions DVV with BCW_1 and BCW_2 provide good results between Reynolds numbers in the range of $0< Re_d \leq 300$. But this conformity gradually deteriorates as the Reynolds number increases. Consequently, the combination of BCW_1 and AWV boundary conditions gives the best conformity with the experimental results among all boundary conditions used presently. Conclusions driven from the present work support conclusions of Mills [9] who stated that the same boundary condition cannot be used for both vertical and horizontal walls in the cylindrical coordinates.

Examining all distributions of the discharge coefficient, maximum difference between numerical results of discharge coefficients computed from various boundary conditions at Reynolds number $Re_d=100$ is approximately 3%. If the similar comparison is done at Reynolds number of $Re_d=1000$, the maximum conformity with the experimental results is provided by the combination of BCW_1 and AWV boundary combinations. On the other hand, the maximum difference between the present results and the experimental results is given by the combination of BCW_2 and SCP boundary conditions.

7. CONCLUSIONS

This study was conducted to investigate the effects of different boundary conditions on the numerical solutions of the laminar flow through the orifce plate inserted in the pipe. Throughout the calculations, the orifice/pipe diameter ratio was taken as $\beta=0.6$ and the orifice plate thickness/diameter ratio L^* was taken as 1/12. Governing equations were converted in the form of vorticity-transport equations and then solved by using alternating direction implicit method.

Among the boundary conditions used in the present work, combination of BCW_1 and AWV boundary conditions gives the best agreement with the experimental results. On the other hand, the maximum discrepancy in comparison with the experimental results is given by the combination of BCW_2 and SCP boundary conditions.

8. NOMENCLATURE

C_d	: Orifice discharge coefficient
d_o	: Diameter of orifice plate
D	: Diameter of pipe
R	: Radius of pipe
L	: Orifice thickness

L^* : Orifice thickness/diameter ratio ($\frac{L}{d_o}$)

P : Pressure

P^* : Dimensionless pressure ($\frac{P}{\frac{1}{2}\rho V_{max}^2}$)

Q : Volume flow rate

r : Radial coordinate

r^* : Dimensionless radial coordinate ($\frac{r}{R}$)

t : Time

t^* : Dimensionless time ($\frac{t\overline{V}}{R}$)

Re_o : Reynolds number based on orifice diameter ($\frac{\rho\overline{V}d_o}{\mu}$)

Re_d : Reynolds number based on pipe diameter ($\frac{\rho\overline{V}D}{\mu}$)

V_r : Radial velocity

V_r^* : Dimensionless radial velocity ($\frac{V_r}{\overline{V}}$)

V_z : Axial velocity

V_z^* : Dimensionless axial velocity ($\frac{V_z}{\overline{V}}$)

V_{max} : Maximum velocity

$\overline{V}$: Average velocity

ω : Vorticity

ω^* : Dimensionless vorticity ($\frac{\omega R}{\overline{V}}$)

z : Axial coordinate

z^* : Dimensionless axial coordinate ($\frac{z}{R}$)

β : Ratio of orifice diameter to the pipe diameter ($\frac{d_o}{D}$)

H : Distance between two grids

Δt : Time step

ρ : Density

ψ : Stream function

ψ^* : Dimensionless stream function ($\frac{\psi}{\overline{V}R^2}$)

9. REFERENCES

1. Morrison, G.L., DeOtte, R.E., Panak, D.L., and Nail, G.H., 1990. "The Flow Inside an Orifice Flow Meter". Chemical Engineering Progress, Vol.86, pp. 75-80.

2. Bohra, L. K., 2004, "Flow and Pressure Drop of Highly Viscous fluids in Small Aperture Orifices". MSc. Thesis. Georgia Institute of Technology**.**

3. Tunay, T., Sahin, B., Akıllı, H., 2004. "Investigation of Laminar and Turbulent flow through an orifice plate inserted in a pipe". Transactions of the Canadian Society for Mechanical Engineering 28 (2B): 403-414.

4. Johansen, F. C., 1930. "Flow Through Pipe Orifices at Low Reynolds Numbers". Proc R Soc, 126 (Series A), 231.

5. Alvi, S. H., Sridharan, K., and Lakshmana Rao, N. S., 1978. "Loss Characteristics of Orifices and Nozzles". Journals of Fluids Engineering, 100, 299-307.

6. Nigro, F. E. B., Strong, A. B., Alpay, S. A., 1978. "A Numerical Study of the Laminar Viscous Incompressible Flow Through a Pipe Orifice". Journal of Fluids Engineering, Vol.100, pp. 467-472.

7. Grose, R. D., (1983). "Orifice Flow at Low Reynolds Number". Journal of Pipelines, Vol. 3(3), pp 207-214.

8. Nallasamy, M., 1986. "Numerical Solution of the Separating Flow Due to an Obstruction". Computers and Fluids, Vol. 14, No. 1, pp. 59-68.

9. Mills, R. D., 1968. "Numerical Solutions of Viscous Flow Through a Pipe Orifice at Low Reynolds Numbers". Mechanical Engineering Science, 10(2), 133-140.

10. Coder, D. A., Buckley, F. T., 1974. "Implicit Solutions of the Unsteady Navier-Stokes Equation For Laminar Flow Through an Orifice Within a Pipe". Computers and Fluids, Vol.2, pp. 295-314.

11. Lester, W. G. S., 1960. "The Flow Past a Pitot Tube at Low Reynolds Numbers". Report and Memoranda Aeronautical Research Committee, No 3240, 1-23.

12. Ma, H., Ruth, D.W., 1994. "A New Scheme for Vorticity Computations Near a Sharp Corner". Computers and Fluids, Vol.23, No.1, pp 23-38.

13. Sahin, B., Ceyhan, H., 1996. "A Numerical and Experimental Analysis of Laminar Flow Through Square Edged Orifice with a Variable Thickness". Transactions of the Institute of Measurement and Control, Vol.18, No.4, pp.166-173.

14. Sahin, B., and Akıllı, H., 1997. "Finite Element Solution of Laminar Flow Through Square-Edged Orifice with a Variable Thickness". International Journal of Computational Fluid Dynamics, Vol.9, pp.85-88.

15. Jones, E. H., Bajura, R. A., 1991. "A Numerical Analysis of Pulsating Laminar Flow Through a Pipe Orifice". Journal of Fluids Engineering, Vol. 113, no. 2, pp. 199-205.

16. Gan, G., Riffat, S. B., 1997. "Pressure Loss Characteristics of Orifice and Perforated Plates". Experimental Thermal and Fluid Science, Vol.14, pp. 160-165.

17. Ramamurthi, K., Nandakumar, K., 1999. "Characteristics of flow through small sharp-edged cylindrical orifices". Flow Measurement and Instrumentation, Vol. 10, pp. 133–143.

18. Huang, H. and Seymour, B. R., 2000. "Finite Difference Solutions of Incompressible Flow Problems with Corner Singularities". Journal of Scientific Computing, Vol. 15, No. 3, pp. 265-292.

19. Mishra, C. and Peles, Y., 2005. "Incompressible and Compressible Flows Through Rectangular Microorifices Entrenched in Silicon Microchannels". Journal of Microelectromechanical Systems, Vol. 14, No. 5, 1000-1012.

20. Zimmermann, H., 1999. "Examination of Disturbed Pipe Flow and Its Effects on Flow Measurement Using Orifice Plates". Flow Measurement and Instrumentation, Vol. 10, pp. 223-240.

21. Erdal, A., Andersson, H. I., 1997. "Numerical Aspects of Flow Computation Through Orifices". Flow Measurement and Instrumentation, Vol. 8, No. 1, pp. 27-37.

22. Chen, J., Wang, B., Wu, B., Chu, Q., 2008. "CFD Simulation of Flow Field in Standard Orifice Plate Flow Meter". Journal of Experiments in Fluid Mechanics, Vol. 22, No. 2, pp. 51-55.

23. Maldonado, J. J. C., Benavides, D. N. M., "Computational Fluid Dynamics (CFD) and Its Application in Fluid Measurement Systems". International Symposium on Fluid Flow Measurement, May 16-18, 2006.